Journal of Materials Chemistry A

Accepted Manuscript

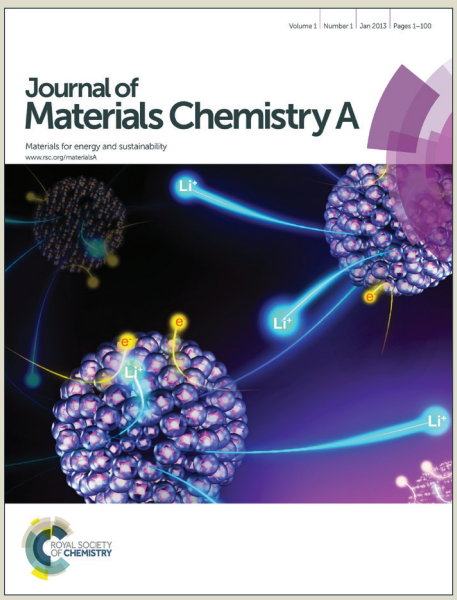

ROYAL SOCIETY OF CHEMISTRY

www.rsc.org/materialsA

Energetics of Lanthanide Cobalt Perovskites: $LnCoO_{3-\delta}$ (Ln = La, Nd, Sm, Gd)

Sulata Kumari Sahu [1], Speranta Tanasescu [2], Barbara Scherrer [3], Cornelia Marinescu [2], Alexandra Navrotsky [1]*

[1]Peter A. Rock Thermochemistry Laboratory and NEAT ORU, University of California Davis, Davis, CA 95616, USA

[2]Institute of Physical Chemistry "Ilie Murgulescu" of the Romanian Academy, Splaiul Independentei 202, 060021 Bucharest, Romania

[3] Nonmetallic Inorganic Materials, ETH Zurich, Zurich, Switzerland

** Corresponding author: anavrotsky@ucdavis.edu*

Abstract

Lanthanide cobalt perovskites $LnCoO_{3-\delta}$ (Ln = La, Nd, Sm, and Gd) are important materials for electroceramics, catalysts, and electrodes in solid oxide fuel cells. Formation enthalpies of $LnCoO_{3-\delta}$ compounds were measured using high temperature oxide melt solution calorimetry. The formation enthalpies of $LaCoO_{2.992}$, $NdCoO_{2.985}$, $SmCoO_{2.982}$ and $GdCoO_{2.968}$ from constituent binary oxides (Ln_2O_3, CoO) and O_2 gas are –111.87 ± 1.36, -98.49 ± 1.33, -91.56 ± 1.46 and -88.16 ± 1.45 kJ/mol, respectively. Thus these perovskites become energetically less stable with decrease in ionic radius of the lanthanide (from La to Gd), which corresponds to a decreasing tolerance factor and increasing oxygen deficiency. The thermodynamic stability of $LaCoO_{2.992}$, $NdCoO_{2.985}$, $SmCoO_{2.982}$ and $GdCoO_{2.968}$ was also assessed considering their oxygen partial pressures for decomposition, with good agreement between thermochemical and equilibrium data.

***Keywords**: Lanthanide perovskite, catalysis, SOFC materials, oxide melt solution calorimetry, formation enthalpy, oxide stability.*

Introduction

Perovskite oxides (ABO_3) have attracted attention due to their subtle structural variations and important physical properties. Lanthanide cobalt perovskites, $LnCoO_3$, have applications as electroceramics, catalysts, solid oxide fuel cell (SOFC) electrodes, chemical sensors, and oxygen separation membranes[1-3]. Their properties are sensitive to the ionic radius of Ln^{3+}, mainly due to the structural distortion induced by bond length misfit in the perovskite structure[4]. These

distortions not only affect the crystal structure, but also influence physical properties such as electrical conductivity, catalytic activity and dielectric properties. Distortion in the perovskite (ABO_3) can be described by the Goldschmidt tolerance factor (*t*), which assesses the fit of the 'A-site' cation in the central site provided by the corner sharing BO_6 octahedra, and is defined by:

$$t = \frac{r_A + r_O}{\sqrt{2}(r_B + r_O)} \quad (1)$$

where r_A, r_B and r_O are the ionic radii of the A-site cation, B-site cation and O^{2-} anion, respectively. Generally, perovskites, with increasing distortion as *t* deviates from unity, occur for $0.75 \leq t \leq 1.0$. At room temperature, crystallographic distortion of $LnCoO_3$ increases with increasing Ln atomic number, i.e. with decreasing Ln^{3+} ionic radius[5]. The tolerance factor, *t* (calculated using the Shannon effective ionic radii for lanthanides in twelvefold coordination and that for high spin Co^{3+} in octahedral coordination[6]), for $LaCoO_3$, $NdCoO_3$, $SmCoO_3$, and $GdCoO_3$ are 0.97, 0.94, 0.93, and 0.92, respectively. In the series from La to Gd, a symmetry change from rhombohedral to orthorhombic has been seen with decreasing size of the A-site cation[7, 8]. $LaCoO_3$ has a rhombohedrally distorted perovskite structure, $NdCoO_3$ an almost cubic structure and the perovskites with Sm and Gd show orthorhombic distortions[9]. In some cases, the structural distortion is accompanied by a spin state transition of the trivalent cobalt ion (Co^{3+}). Co ions have different ionic radii in different spin states; hence change in spin state of Co^{3+} results in change in the octahedral Co-O bond length and corresponding change in the volume of the unit cell and the tolerance factor[10, 11]. There has been much discussion in the literature of spin transitions in lanthanide cobaltites; the situation is complicated by gradual transitions and the occurrence of intermediate spin, as well as low spin and high spin states[9]. These transitions begin

below or at room temperature. For consistency, we have used the high spin state as reference for ionic radii of all the lanthanides in our discussion below.

It has been reported that lanthanide cobaltites exhibit small oxygen deficiency[12]. Thermogravimetric investigations of $La_{1-x}Sr_xCoO_{3-\delta}$ in the range of $10^{-5} \leq P_{O2}$ / (atm) ≤ 1 and 573 – 1273 K indicate the oxygen non-stoichiometry, δ, increases with increasing temperature, increasing Sr concentration and decreasing oxygen partial pressure[13]. At room temperature, δ for $La_{1-x}Sr_xCoO_{3-\delta}$ in air is close to zero and below 1073 K, δ of $LaCoO_{3-\delta}$ is not detectable[13]. No oxygen excess compositions have been reported for lanthanide perovskites except for $LnMnO_{3+\delta}$ [14].

Different thermodynamic techniques have been employed to determine the stability of the rare earth based ternary oxides [15-17]. The Gibbs free energies and enthalpies of formation of multicomponent transition metal oxides were obtained using solid electrolyte based galvanic cell methods and calorimetric techniques[18-25]. The stability of lanthanide cobaltite perovskites was also determined by thermogravimetry by considering the decomposition reaction, $LnCoO_3 \rightarrow Ln_2O_3 + CoO + ½\ O_2$ (g) in a reducing atmosphere[14]. Recent studies on oxygen deficient lanthanide cobaltites, $LnCoO_{3-\delta}$ ($LaCoO_{2.992}$, $NdCoO_{2.985}$, $SmCoO_{2.982}$ and $GdCoO_{2.968}$), suggest that their conductivity in the semiconducting state and activation energy for the transition to metallic conduction decrease monotonically with increasing ionic radius of the Ln cation[9]. The thermodynamic stability against reduction and the conductivity of the rare earth cobaltites correlate with the oxygen non-stoichiometry, δ, of $LnCoO_{3-\delta}$. $LaCoO_{2.992}$ has the lowest oxygen non-stoichiometry and appears to have the highest thermodynamic stability, whereas $GdCoO_{2.968}$ has the highest oxygen non-stoichiometry and appears to have the lowest thermodynamic stability [9].

The present study reports enthalpies of formation measured by high temperature oxide melt solution calorimetry for several lanthanide cobalt oxide perovskites, discusses their thermodynamic stability as a function of lanthanide element and oxygen non-stoichiometry and correlates their catalytic properties to their thermodynamic stability. The thermochemical calculations are carried out using (I) the nominal compositions (II) the analyzed compositions from microprobe experiments, and (III) the oxygen deficient non-stoichiometric compositions. This allows us to conclude that different assumptions concerning these compositional variables do not change the thermochemical properties significantly.

Experimental methods

$LnCoO_{3-\delta}$ ($LaCoO_{2.992}$, $NdCoO_{2.985}$, $SmCoO_{2.982}$ and $GdCoO_{2.968}$) were synthesized via the combined citric acid and ethylene diamine tetraacetic acid (EDTA) complexing method, detailed elsewhere[9]. Briefly, EDTA solution were prepared by dissolving EDTA (Acros Organics, ACS reagent) in a 25 % aqueous ammonia solution (Merck, p.a.). lanthanide nitrates; $La(NO_3)_3$, $Nd(NO_3)_3$, $Sm(NO_3)_3$ (Sigma- Aldrich, 99.9 %), $Gd(NO_3)_3$ (ABCR, 99.9 %) and cobalt nitrate, $Co(NO_3)_2$ (Fluka, ≥ 98 %) were dissolved in water after determining the exact water content of the starting materials. A clear nitrate solution and citric acid monohydrate (Fluka, ≥ 99.5 %) were added to the EDTA solution under stirring and the solution were heated in an oil bath at 353 - 413 K for 12 h. The resulting dark brown foam was then calcined in a furnace at 1373 K for 2 h in air.

Phase purity of the synthesized samples was analyzed by powder X-ray diffraction (XRD). Patterns were recorded using a Bruker D8 Advance diffractometer (Bruker-AXS Inc.) operated at an accelerating voltage of 40 kV and an emission current of 40 mA with CuKα

radiation (λ = 0.15406 nm). Data were acquired from 10 to 70 ° 2θ with a step size of 0.03 ° and a collection time of 0.5 s/step.

The oxygen non-stoichiometry (δ*)* of the perovskites $LnCoO_{3-\delta}$ was obtained from the measured mass loss in a reducing atmosphere (5 vol. % H_2 in He) from 303 K to 1123 K using a Netzsch STA 449 thermal analyzer detailed elsewhere[9]. Briefly, all perovskites started to decompose at ~623 K in the reducing atmosphere. At higher temperatures (>623 K), pronounced mass losses occurred until a stable mass of roughly 91 wt. % was reached at 923 ± 50 K. The mass losses occur in two steps according to the reaction:

$$LnCoO_{3-\delta} \rightarrow \tfrac{1}{2}\, Ln_2O_3 + CoO + (0.5 - \delta)/2\ O_2 \rightarrow \tfrac{1}{2}\, Ln_2O_3 + Co + (1.5 - \delta)/2\ O_2 \qquad (2)$$

In the first step, the lanthanide cobaltite decomposes into the corresponding lanthanide oxide and cobalt (II) oxide. In the second step, the cobalt (II) oxide is reduced to metallic cobalt. The non-stoichiometry (δ) in $LnCoO_{3-\delta}$ is determined from the observed mass loss in TGA measurements and the uncertainties in δ were obtained by propagating the uncertainties in mass change. Obtained δ values for $LaCoO_{3-\delta}$, $NdCoO_{3-\delta}$, $SmCoO_{3-\delta}$ and $GdCoO_{3-\delta}$ are 0.0081 ± 0.0002, 0.0152 ± 0.0003, 0.0179 ± 0.0003, and 0.0318 ± 0.0008; respectively. The calculation of oxygen non-stoichiometry of the original perovskites is based on the total decomposition reaction and the masses measured at 473 and 1073 K. In the rest of the manuscript, $LnCoO_{3-\delta}$ has been presented as $LaCoO_{2.992}$, $NdCoO_{2.985}$, $SmCoO_{2.982}$ and $GdCoO_{2.968}$, by rounding off the oxygen non-stoichiometry to three decimal places without indicating the uncertainties, which are in the fourth place.

The compositions (Ln/Co ratios) of the synthesized samples were measured using wavelength dispersive electron microprobe analysis with a Cameca SX100 instrument operated

at an accelerating voltage of 15 kV, a beam current of 20 nA, and a beam size of 1 μm. Sample homogeneity was investigated using back-scattered electron images. For the microprobe analysis, powders were pelletized and annealed at 1073 K. The sintered pellets were polished and carbon-coated. Co metal and lanthanide orthophosphate standards were used. The compositions were calculated from an average of 10 data points per sample and the uncertainties were calculated as two standard deviations of the mean.

High temperature oxide melt drop solution calorimetry was performed in a custom-made isoperibol Tian-Calvet twin microcalorimeter described previously[24, 26-28]. The calorimeter was calibrated against the heat content of 5 mg pellets of high purity α-Al_2O_3 (99.997 %). The calorimetric assembly was flushed with oxygen at 43 ml/min with oxygen bubbling through the solvent at 4.5 ml/min to aid dissolution. The experiments were also carried out using high purity argon as flushing and bubbling gas. ~5 mg sample pellets were loosely pressed, weighed and dropped from room temperature into $3Na_2O{\cdot}4MoO_3$ solvent in a platinum crucible at 1075 K in the calorimeter. The final state was CoO and Ln_2O_3 dissolved in sodium molybdate in both oxygen and argon environments[29-31]. Transposed temperature drop calorimetry (no solvent present) was performed using the same calorimeter to determine the enthalpy increment of $LnCoO_{3-\delta}$ from room temperature to 1075 K.

Results and Discussion

XRD analyses of $LaCoO_{2.992}$, $NdCoO_{2.985}$, $SmCoO_{2.982}$ and $GdCoO_{2.968}$ confirm the phase purity of the samples, with pseudo-cubic lattice constants of 3.831 ± 0.003, 3.773 ± 0.003, 3.76 ± 0.002, and 3.74 ± 0.002 Å, respectively. The microprobe analyses confirm that the samples are generally stoichiometric with respect to metal content within experimental error and the Ln/Co

ratios are 1.018 ± 0.003, 1.018 ± 0.004, 0.984 ± 0.012 and 1.012 ± 0.017 for La/Co, Nd/Co, Sm/Co and Gd/Co, respectively. One can write the microprobe compositions of the Ln-cobaltites from the exact analyzed compositions of lanthanides, cobalt and with three oxygen atoms per formula unit as; $La_{1.009\pm0.002}Co_{0.991\pm0.002}O_{3.000\pm0.006}$, $Nd_{1.009\pm0.003}Co_{0.991\pm0.003}O_{3.000\pm0.010}$, $Sm_{0.992\pm0.008}Co_{1.008\pm0.009}O_{3.000\pm0.025}$, and $Gd_{1.006\pm0.012}Co_{0.994\pm0.012}O_{3.000\pm0.035}$. The compositions were calculated from an average of 10 data points per sample and the uncertainties were calculated as two standard deviations of the mean. No secondary phases were observed on the back-scattered electron images of the sintered samples.

The thermochemical calculations were carried out using (I) the nominal compositions (II) the analyzed compositions from microprobe experiments, and (III) the oxygen deficient nonstoichiometric compositions, as discussed in the previous section. This allowed us to conclude that the different assumptions of these compositional variables do not change the thermochemical properties significantly.

The enthalpies of drop solution, $\Delta_{ds}H$, of Ln-cobaltites are shown in Table 1. The enthalpies of formation from component oxides and elements were obtained using thermodynamic cycles shown in Table 2. Similarly, different appropriate balanced thermochemical cycles were used to derive the formation enthalpies of Ln-cobaltites with microprobe compositions and with nominal compositions. For a given Ln-cobaltite perovskite, the drop solution enthalpy of nominal, microprobe and oxygen non-stoichiometric compositions were calculated based on their formula weights.

The enthalpy of drop solution of binary oxides, La_2O_3, Nd_2O_3, Sm_2O_3, and Gd_2O_3 and CoO in $3Na_2O{\cdot}4MoO_3$ at 1075 K were taken from prior measurements[32, 33]. For calculation of enthalpies of formation from the elements, the enthalpies of formation of binary oxides from

Robie *et al*. were used[34]. The calculated formation enthalpies from corresponding oxides, (Ln_2O_3, CoO) plus O_2 gas at 298 K, $\Delta_f H^{ox}$, for $LaCoO_{2.992}$, $NdCoO_{2.985}$, $SmCoO_{2.982}$ and $GdCoO_{2.968}$ are shown in Table 1. Similarly, $\Delta_f H^{ox}$ of perovskites with nominal compositions and microprobe compositions were determined from the appropriate thermochemical cycles and are shown in Table 1. The calculated $\Delta_f H^{ox}$ from constituent oxides and oxygen gas of Ln-cobaltites with nominal compositions, measured oxygen non-stoichiometric compositions, and the microprobe compositions are the same within the reported uncertainties (Table 1). The calculated formation enthalpies for $LaCoO_{2.992}$, $NdCoO_{2.985}$, $SmCoO_{2.982}$ and $GdCoO_{2.968}$ from elements are given in Table 3). These are the first set of experimental data on enthalpies of formation for Ln-cobaltites derived by solution calorimetry.

The obtained enthalpy increments ($H_{1075\ K}$-$H_{298\ K}$) for $LaCoO_{2.992}$, $NdCoO_{2.985}$, $SmCoO_{2.982}$ and $GdCoO_{2.968}$ are reported in Table 3. The measured enthalpy increments ($H_{1075\ K}$-$H_{298\ K}$) generally compare reasonably well (agreement within 6 % or better) with the reported values by Patil *et al.*[16, 35] from heat capacity measurements (Table 3). Because $LaCoO_{2.992}$, $NdCoO_{2.985}$, $SmCoO_{2.982}$ and $GdCoO_{2.968}$ are only slightly oxygen deficient, the configurational entropy terms arising from mixing of oxygen ions and vacancies on the oxide sublattice and of Co^{2+} and Co^{3+} on octahedral sites can be neglected. The entropy of formation of $LnCoO_{3-\delta}$ (s) from elements Ln (s), Co(s) and O_2 (g) at 298 K were determined by combining the Gibbs energy of formation of $LnCoO_3$ reported in the literature[35] from electrochemical measurements and enthalpy of formation from constituent elements in the present calorimetric work (Table 3). The obtained formation enthalpies and entropies at 298 K for $LaCoO_{2.992}$, and $SmCoO_{2.982}$ compares well with those reported by Patil et al[35]. However for $NdCoO_{2.985}$ and $GdCoO_{2.968}$, differences of 20 - 30 kJ/mol for $\Delta_f H°$ and about 100 J/(Kmol) for $\Delta_f S°$, were seen. It has to be noted that uncertainties

of the reported $\Delta_f H°_m$ (298 K) values[35] were not provided. Patil et al[35] calculated $\Delta_f H°_m$ (298 K) from the reported $\Delta_f G°_m$ ($LnCoO_3$, s, T), the enthalpy of the electronic transition of $LnCoO_3$, the electronic transition temperature, and heat capacity for Ln (s), Co(s), and O_2 (g) and $LnCoO_3$ using appropriate relations. Bringing down the $\Delta_f H°_m$ at the mean temperature of the e.m.f. measurements (from which $\Delta_f G°_m$ of $LnCoO_3$, were determined) to room temperature, can be associated with larger uncertainties. Again the uncertainties in the values of $\Delta_f H°_m$ (298 K) carry the uncertainties involved in all terms. The difference of 20 - 30 kJ/mol for $\Delta_f H°_m$ (298 K) is in agreement within 2 %, which might be within the uncertainties of the $\Delta_f H°_m$ (298 K) value reported by Patil et al[35]. It must be pointed out that the difference of 2 % in $\Delta_f H^0$ for $NdCoO_3$ and $GdCoO_3$, leads to 30 % difference in $\Delta_f S^0$. However, we believe, even the propagated uncertainty in going from enthalpy to entropy is high, it is useful to have a comparison. Furthermore we note that it is difficult to assign absolute errors to the temperature slope of electrochemical data because there can be potential sources of systematic error and the temperature range of measurements is frequently small.

The Gibbs free energies of the reaction ($\Delta_f G^{rxn}$), $LnCoO_3 \rightarrow ½\ Ln_2O_3 + CoO + ¼\ O_2$, were reported over a wide range of temperatures by electromotive force (e.m.f.) methods[15, 17, 35, 36]. From the reported $\Delta_f G^{rxn}$, enthalpies of reactions ($\Delta_f H^{ox}$) at the mean temperature of the e.m.f. measurements were determined (Table 4). In the present work, $\Delta_f H^{ox}$ at the mean temperature of the e.m.f. measurements was calculated by adding the necessary enthalpy increment terms to the $\Delta_f H^{ox}$ at room temperature determined by the calorimetric techniques, as follows

$$\Delta_f H^{ox}_{TK}\langle LnCoO_3\rangle = \Delta_f H^{ox}_{298.15K}\langle LnCoO_3\rangle + \int_{298.15K}^{TK} \Delta C_p dT \qquad (3)$$

where, $\Delta_f H^{ox}_{TK} < LnCoO_3 >$ is the calorimetrically determined formation enthalpies of lanthanide cobaltites at the mean temperature of e.m.f measurements, $\Delta_f H^{ox}_{298.15K} < LnCoO_3 >$ is the enthalpies of formation at room temperature determined by calorimetric techniques. $\int_{298.15K}^{TK} \Delta C_p dT$ is the enthalpy increment term. ΔC_p is the difference in the heat capacities of $LnCoO_3$ and its constituent oxides and oxygen gas, (½ Ln_2O_3+ CoO+ ¼ O_2). $\int_{298.15K}^{TK} \Delta C_p dT$ were calculated as follows,

$$\int_{298.15K}^{TK} \Delta C_p dT = \int_{298.15K}^{TK} \left[C_p^{LnCoO_3} - \left((1/2) C_P^{Ln_2O_3} + C_P^{CoO} + (1/4) C_P^{O_2} \right) \right] dT = \int_{298.15K}^{T_1 K} \Delta C_p dT + \Delta_{tr} H_{LnCoO_3} + \int_{T_1 K}^{TK} \Delta C_p dT \quad (4)$$

In equation (4), T_1 is the electronic transition temperature of the Ln-cobaltites; $\Delta_{tr} H_{LnCoO_3}$. T_1 for $LaCoO_3$, $NdCoO_3$, $SmCoO_3$ and $GdCoO_3$ are 554 K, 610 K, 619 K, and 675 K with an uncertainty of ±2 K, respectively[16]. The heat capacity and electronic transition enthalpies of $LaCoO_3$, $NdCoO_3$, $SmCoO_3$ and $GdCoO_3$ were taken from Patil *et al.*[16]. The heat capacity expression of corresponding binary oxides and oxygen gas were taken from Pankratz[37]. Calculated enthalpies of formations of $LnCoO_3$ from the constituent oxides plus O_2 gas by calorimetric technique and e.m.f. techniques are reported in Table 4. The obtained $\Delta_f H^{ox}$ for $LaCoO_{2.992}$, and $GdCoO_{2.982}$ compares well with those reported by Patil et al[35]. However for $NdCoO_3$ and $SmCoO_3$, differences of about 20 kJ/mol was observed, which can be explained based on the associated error in $\Delta_f G^{rxn}$ (T), from which $\Delta_f H^{ox}$ is derived. Patil et al[35] derermined a single $\Delta_f G^{rxn}$ (T) expression for each $LnCoO_3$ system by combined the data reported by previous investigators, separately by least squares analysis method in the temperature range 1000 – 1500 K. We believe such methods of calculation of $\Delta_f G^{rxn}$ (T) can have large error, which in turn will be reflected in $\Delta_f H^{ox}$ of $LnCoO_3$. Hence, again we suggest that the associated error in the $\Delta_f G^{rxn}$

(T) will accommodate the observed difference of the calculated and reported values $\Delta_f H^{ox}$.

Scherrer *et al.*[9] determined thermodynamic stability of $LnCoO_{3-\delta}$ perovskites from the Gibbs free energy change corresponding to decomposition of $LnCoO_{3-\delta}$ perovskites ($\Delta_d G^0$) for reaction (2) employing an e.m.f. technique, where 12.84 wt.% yttria stabilized zirconia (YSZ) and Fe/FeO served as the solid electrolyte and reference electrode, respectively. The obtained oxygen partial pressure (P_{O_2}) at 1123 K corresponding to the decomposition reaction (2) are plotted against the oxygen non-stoichiometry δ of $LnCoO_{3-\delta}$ (Fig. 1). Also the $\Delta_f H^{ox}$ values of $LnCoO_{3-\delta}$, determined by calorimetry in the present work are plotted against the non-stoichiometry δ of $LnCoO_{3-\delta}$ (Fig. 1). With increase in non-stoichiometry, the formation enthalpy becomes less exothermic and the oxygen partial pressure for the decomposition of the $LnCoO_{3-\delta}$ increases. For the compounds with smaller radii of the Ln cation, the non-stoichiometry δ and log P_{O_2} are higher and the formation enthalpy is less exothermic and therefore the thermodynamic stability is lower. Hence based on the present investigation and previous literature information[9], it can be concluded that the thermodynamic stability as well as the oxygen non-stoichiometry in $LnCoO_{3-\delta}$, depend on the crystal structure, which is specified through the tolerance factor and distortion which determines the Co–O–Co bond angle.

Figure 2a depicts the variation of formation enthalpy of $LnCoO_{3-\delta}$ from their constituent oxides plus oxygen with ionic radius of the lanthanide ions (Ln^{3+}). They become more endothermic with decrease in ionic radius of the lanthanides, which corresponds to decrease of the Goldschmidt tolerance factor (*t*) (Fig. 2b). Thus the largest ion in the lanthanide series forms the most stable perovskite.

It is clear from the present investigation that for compounds with smaller Ln^{3+}radii, the non-stoichiometry δ is higher and the formation enthalpy is less exothermic and therefore the thermodynamic stability is lower. However the individual contribution of non-stoichiometry and lanthanide cation size to the overall thermodynamic stability can not be separated at present.

According to the literature data on basicity of Ln_2O_3[38], with increase in size of the lanthanide ions, the basicity increases in the order $Gd_2O_3 < Sm_2O_3 < Nd_2O_3 < La_2O_3$. Since this is the same order as increasing ionic radius, it is clear that thermodynamic stability of the Ln-cobaltite perovskite increases with increasing basicity of the lanthanide oxide, or increasing difference in basicity between the lanthanide oxide and cobalt oxide.

The observed trend on energetics of lanthanide cobaltite perovskites in the present work compares well with energies of the reduction reaction; $LnCoO_3 \rightarrow 0.5\ Ln_2O_3 + CoO + ½\ O_2$ (g), observed by Lago et al.[38] and Arakawa *et al.*[39]. The reduction reactions were assumed to be thermodynamically controlled. Among the considered series, $LaCoO_3$, with highest thermodynamic stability, reduces at the highest temperatures[38]. Reoxidation of cobalt to form the parent perovskite structure is thermodynamically more favorable for larger lanthanides[38].

The Gibbs free energy of the reaction; $0.5\ Ln_2O_3 + CoO + ½\ O_2$ (g) $\rightarrow LnCoO_3$, at 1273 K measured by Patil *et al.*[16] indicates a linear change with the ionic radius of the lanthanide elements with 12 coordination. The value for $LaCoO_3$ fits well despite the difference of the crystal system from other $LnCoO_3$ perovskite structures, suggests that the crystal system has a smaller effect on ΔG^{rxn} than the ionic radius. E.m.f. studies and heat capacity measurements revealed the presence of first order endothermic phase transformation of $LaCoO_3$ at 1212 K with $\Delta_{tr}H = 15.275$ kJ/ mol [16, 40].

The observed energetic trend of the lanthanide cobaltite perovskites, where stability increases in the order $GdCoO_{2.968}$ < $SmCoO_{2.982}$ < $NdCoO_{2.958}$ < $LaCoO_{2.992}$ can elucidate the observed trends of their physical properties. The catalytic activity of $LnCoO_3$ (which depends on easy reduction of its cobalt ion to metallic cobalt) increases in the order $LaCoO_3$ < $NdCoO_3$ < $SmCoO_3$ < $GdCoO_3$[38, 41]. The thermodynamically less stable $GdCoO_{2.968}$ favors easier reduction of Co^{3+} to metallic cobalt (Co) on the surface of Gd_2O_3. On the other hand, the most stable perovskite $LaCoO_{2.992}$, disfavors the reduction of Co^{3+} to Co and this limits the catalytic activity. Analogous trends were observed by Lago *et al.*[38] where Gd yields the highest quantities of CO and H_2 from methane, whereas with the catalyst containing La, no syngas formation was observed.

Conclusions

Energetics of lanthanide cobaltite perovskites (Ln = La, Nd, Sm, Gd) have been determined for the first time employing oxide melt solution calorimetry. Enthalpies of formation of the $LnCoO_{3-\delta}$ perovskites from their constituent oxides become less exothermic with decrease in the ionic radius of lanthanides and increase in oxygen non-stoichiometry. The thermodynamic stability correlates well with that expected from their tolerance factors and oxygen partial pressures corresponding the decomposition.

Acknowledgments

A.N. and S.K.S. thank the U.S. Department of Energy, Office of Basic Energy Sciences, grant DE-FG02-03ER46053 for support of the calorimetric studies. The authors thank Ludwig J.

Gauckler and Julia Martynczuk from the Nonmetallic Inorganic Materials Group of ETH Zurich (Switzerland) and to Florentina Maxim from the Institute of Physical Chemistry, Bucharest (Romania) for the materials synthesis within the Joint Research Project No. IZ73Z0 128185/1 of the Swiss National Science Foundation program: Scientific Co-operation between Eastern Europe and Switzerland (SCOPES 2009-2012).

References

1. T. Arakawa, H. Kurachi and J. Shiokawa, *Appl Phys Lett*, 1985, **47**, 1183-1184.
2. D. D. Sarma and C. N. R. Rao, *J. Electron Spectrosc*, 1980, **20**, 25-45.
3. S. Ricote, N. Bonanos, F. Lenrick and R. Wallenberg, *J Power Sources*, 2012, **218**, 313-319.
4. V. M. Goldschmidt, *Naturwissenschaften*, 1926, **14**, 477-485.
5. S. V. Kurgan, G. S. Petrov, L. A. Bashkirov and A. I. Klyndyuk, *Inorg Mater*, 2004, **40**, 1224-1228.
6. R. D. Shannon, *Acta Crystallogra A*, 1976, **32**, 751-767.
7. J. Q. Yan, J. S. Zhou and J. B. Goodenough, *Phys Rev B*, 2004, **69**, 014402:1-5.
8. Y. Sadaoka, E. Traversa and M. Sakamoto, *J Mater Chem*, 1996, **6**, 1355-1360.
9. B. Scherrer, A. S. Harvey, S. Tanasescu, F. Teodorescu, A. Botea, K. Conder, A. N. Grundy, J. Martynczuk and L. J. Gauckler, *Phys Rev B*, 2011, **84**, 085113:1-9.
10. G. Thornton, B. C. Tofield and A. W. Hewat, *J Solid State Chem*, 1986, **61**, 301-307.
11. S. Stolen, *J Chem Thermodyn*, 1998, **30**, 1495-1507.
12. N. B. Ivanova, S. G. Ovchinnikov, M. M. Korshunov, I. M. Eremin and N. V. Kazak, *Phys Usp*, 2009, **52**, 789-810.

13. J. Mizusaki, Y. Mima, S. Yamauchi, K. Fueki and H. Tagawa, *J. Solid State Chem.*, 1989, **80**, 102-111.

14. T. Nakamura, G. Petzow and L. J. Gauckler, *Mater Res Bull*, 1979, **14**, 649-659.

15. A. Patil, S. Dash, S. C. Parida and V. Venugopal, *J Alloys Compd*, 2004, **384**, 274-278.

16. A. Patil, S. C. Parida, S. Dash and V. Venugopal, *Thermochim Acta*, 2007, **465**, 25-29.

17. A. N. Petrov, V. A. Cherepanov, A. Y. Zuyev and V. M. Zhukovskii, *J Solid State Chem*, 1988, **77**, 1-14.

18. S. K. Sahu, R. Ganesan and T. Gnanasekaran, *J Nucl Mater*, 2008, **376**, 366-370.

19. S. K. Sahu, R. Ganesan and T. Gnanasekaran, *J Chem Thermodyn*, 2010, **42**, 1-7.

20. S. K. Sahu, R. Ganesan and T. Gnanasekaran, *J Nucl Mater*, 2012, **426**, 214-222.

21. S. K. Sahu, R. Ganesan and T. Gnanasekaran, *J Chem Thermodyn*, 2013, **56**, 57-59.

22. S. K. Sahu, R. Ganesan, V. Jayaraman and T. Gnanasekaran, *Mater Sci Forum*, 2012, **710**, 751-756.

23. S. K. Sahu, R. Ganesan, T. G. Srinivasan and T. Gnanasekaran, *J Chem Thermodyn*, 2011, **43**, 750-753.

24. S. K. Sahu and A. Navrotsky, High-Temperature Materials Chemistry and Thermodynamics, in High Temperature Materials and Mechanisms, CRC Press, 2014, pp. 17-38.

25. S. K. Sahu, M. Sahu, R. S. Srinivasa and T. Gnanasekaran, *Monatsh Chem*, 2012, **143**, 1207-1214.

26. A. Navrotsky, *Phys Chem Miner*, 1997, **24**, 222-241.

27. S. K. Sahu, P. S. Maram and A. Navrotsky, *J Am Ceram Soc*, 2013, **96**, 3670-3676.

28. S. Zlotnik, S. K. Sahu, A. Navrotsky and P. M. Vilarinho, *Chem - Eur J.*, 2015, **21**, 5231-5237.

29. T.R.S. Prasanna, A. Navrotsky, *J Solid State Chem*, 1994, **112**, 192-195.

30. M. Wang, *Solid State Ionics*, 2004, **166**, 167-173.

31. N. H. Perry, T. O. Mason, C. Ma, A. Navrotsky, Y. Shi, J. S. Bettinger, M. F. Toney, T. R. Paudel, S. Lany and A. Zunger, *J Solid State Chem*, 2012, **190**, 143-149.

32. A. Navrotsky, *J Am Ceram Soc*, 2014, **97**, 3349-3359.

33. M. G. A. Mielewczyk-Gryn, A.Navrotsky, *Manuscript under preparation*, 2015.

34. B. S. H. R. A. Robie, and J. R. Fisher,, *Thermodynamic Properties of Minerals and Related Substances at 298.15 K and 1 Bar (105 Pascals) Pressure and at Higher Temperatures*, U.S. Geological Survey, Reston, VA, 1995.

35. A. Patil, S. Dash, S. C. Parida and V. Venugopal, *Thermochim Acta* 2009, **481**, 7-11.

36. A. N. Petrov, V. A. Cherepanov and A. Y. Zuev, *Zh Fiz Khim*, 1987, **61**, 630-637.

37. L. B. Pankratz, *Bull. - U. S., Bur. Mines*, 1982, **672**, pp 515.

38. R. Lago, G. Bini, M. A. Pena and J. L. G. Fierro, *J Catal*, 1997, **167**, 198-209.

39. T. Arakawa, K. I. Takada, Y. Tsunemine and J. Shiokawa, *Mater Res Bull*, 1989, **24**, 395-402.

40. O. M. Sreedharan and M. S. Chandrasekharaiah, *Mater Res Bull*, 1972, **7**, 1135-1141.

41. A. T. Ashcroft, A. K. Cheetham, J. S. Foord, M. L. H. Green, C. P. Grey, A. J. Murrell and P. D. F. Vernon, *Nature*, 1990, **344**, 319-321.

List of Tables

List of Figures

Figure 1. Non-stoichiometry δ of $LnCoO_{3-\delta}$, oxygen partial pressure[9] at 1123 K and formation enthalpy of $LnCoO_{3-\delta}$ from oxides ($\Delta_f H^{ox}$).

Figure 2a. Formation enthalpies of $LaCoO_{3-\delta}$, $NdCoO_{3-\delta}$, $SmCoO_{3-i}$ and $GdCoO_{3-\delta}$ versus ionic radius of the lanthanides[6].

Figure 2b. Formation enthalpies of $LaCoO_{3-\delta}$, $NdCoO_{3-\delta}$, $SmCoO_{3-\delta}$ and $GdCoO_{3-\delta}$ versus tolerance factor of the lanthanides.

Tables

Table -1

Lanthanide cobaltites	Drop solution enthalpies, $\Delta_{ds}H^{*}$, kJ/mol	Formation enthalpies $\Delta_{f}H^{ox}$, kJ/mol
$LaCoO_3$	28.73±0.34	-111.78±1.36
$LaCoO_{2.992}$	28.72±0.34	-111.87±1.36
$La_{1.009\pm0.002}Co_{0.991\pm0.002}O_{3.000\pm0.006}$	28.83±0.34	-113.40±1.45
$NdCoO_3$	47.77±1.05	-98.33±1.33
$NdCoO_{2.985}$	47.73±1.05	-98.49±1.33
$Nd_{1.009\pm0.003}Co_{0.991\pm0.003}O_{3.000\pm0.010}$	47.73±1.05	-99.36±1.34
$SmCoO_3$	53.25±0.86	-91.39±1.46
$SmCoO_{2.982}$	53.19±0.86	-91.56±1.46
$Sm_{0.992\pm0.008}Co_{1.008\pm0.009}O_{3.000\pm0.025}$	53.83±0.91	-90.34±1.48
$GdCoO_3$	48.45±0.95	-87.83±1.45
$GdCoO_{2.968}$	48.36±0.95	-88.16±1.45
$Gd_{1.006\pm0.012}Co_{0.994\pm0.012}O_{3.000\pm0.035}$	48.55±0.95	-88.51±1.46

*The uncertainties were calculated as two standard deviations of the reported mean value

Table 2

	#Eq	Reactions	Enthalpies (KJ/mol)
From Oxides	1	Ln_2O_3 (xl, 298 K) → Ln_2O_3 (sol^n, 1075 K)	ΔH_1
	2	CoO (xl, 298 K) → CoO (sol^n, 1075 K)	ΔH_2
	3	O_2 (g, 298 K) → O_2 (g, 1075 K)	ΔH_3[34]
	4	$LnCoO_{3-\delta}$ (xl, 298 K) → ½ Ln_2O_3 (sol^n, 1075 K) + CoO (sol^n, 1075 K)+(1-2δ)/4 O_2 (sol^n, 1075 K)	ΔH_4
	5	½ Ln_2O_3 (xl, 298 K) + CoO (xl, 298 K) + (1-2δ)/4 O_2 → $LnCoO_{3-\delta}$ (xl, 298 K)	ΔH_5= ½ ΔH_1+ΔH_2+(1-2δ)/4 ΔH_3-ΔH_4
From elements	6	Co(xl, 298 K) + ½ O_2(g, 298 K) → CoO(xl, 298 K)	ΔH_6
	7	2Ln(xl, 298 K) + 3/2 O_2(g, 298 K) → Ln_2O_3(xl, 298 K)	ΔH_7
	8	Ln (xl, 298 K) + Co (xl, 298 K) + (3- δ) /2 O_2 → $LnCoO_{3-\delta}$ (xl, 298 K)	ΔH_8= ΔH_5+ ΔH_6+ ½ ΔH_7

Where xl = crystalline, sol^n = solution

Table 3.

Compound	Enthalpies of formation, kJ/mol from elements	Enthalpy increments ($H_{1073\ K}$-$H_{298\ K}$), kJ/mol	Formation entropies at 298 KJ/(K. mol)
$LaCoO_{2.992}$	-1247.68 ± 2.71 -1250.2[35]	108.14 ± 0.77 113.7[35]	-294.08 -302.53[35]
$NdCoO_{2.985}$	-1241.62 ± 3.53 -1271.3[35]	114.56 ± 1.69 109.1[35]	-218.41 -317.96[35]
$SmCoO_{2.982}$	-1246.83 ± 4.90 -1249.0[35]	124.86 ± 0.99 125.9[35]	-298.27 -305.55[35]
$GdCoO_{2.968}$	-1235.45 ± 8.75 -1256.8[35]	99.04 ± 1.18 105.5[35]	-229.58 -301.19[35]

Table 4: Comparison of enthalpies of formation of $LnCoO_3$

Samples	Temp./K	$\Delta_f H^{ox}$ Calorimetry (kJ/mol)	$\Delta_f H^{ox}$ Petrov et al[17, 36] (kJ/mol)	$\Delta_f H^{ox}$ Patil et al[15, 35] (kJ/mol)
$LaCoO_3$	1141.5	-109.38 ± 1.85	-120	--
	1250	-107.07 ± 1.85	--	-110.5
$NdCoO_3$	1141.5	-80.44 ± 2.24	-79.02	--
	1250	-78.39 ± 2.24	--	-100.7
$SmCoO_3$	1141.5	-71.62 ± 2.75	-70.83	--
	1250	-70.04 ± 2.75	--	-92.4
$GdCoO_3$	1141.5	-63.70 ± 2.50	-65.04	--
	1250	-61.79 ± 2.50	--	-65.04

Figure 1

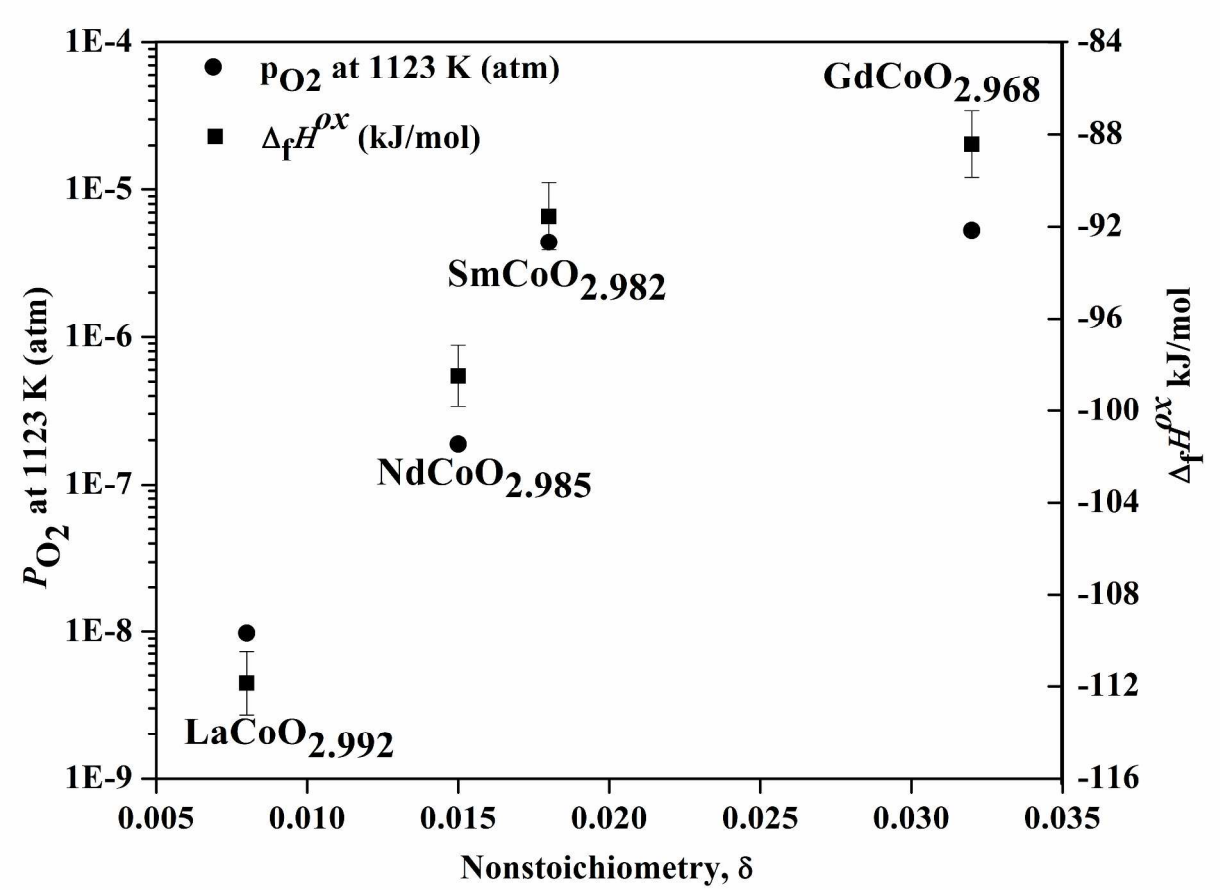

Figure 2 (a)

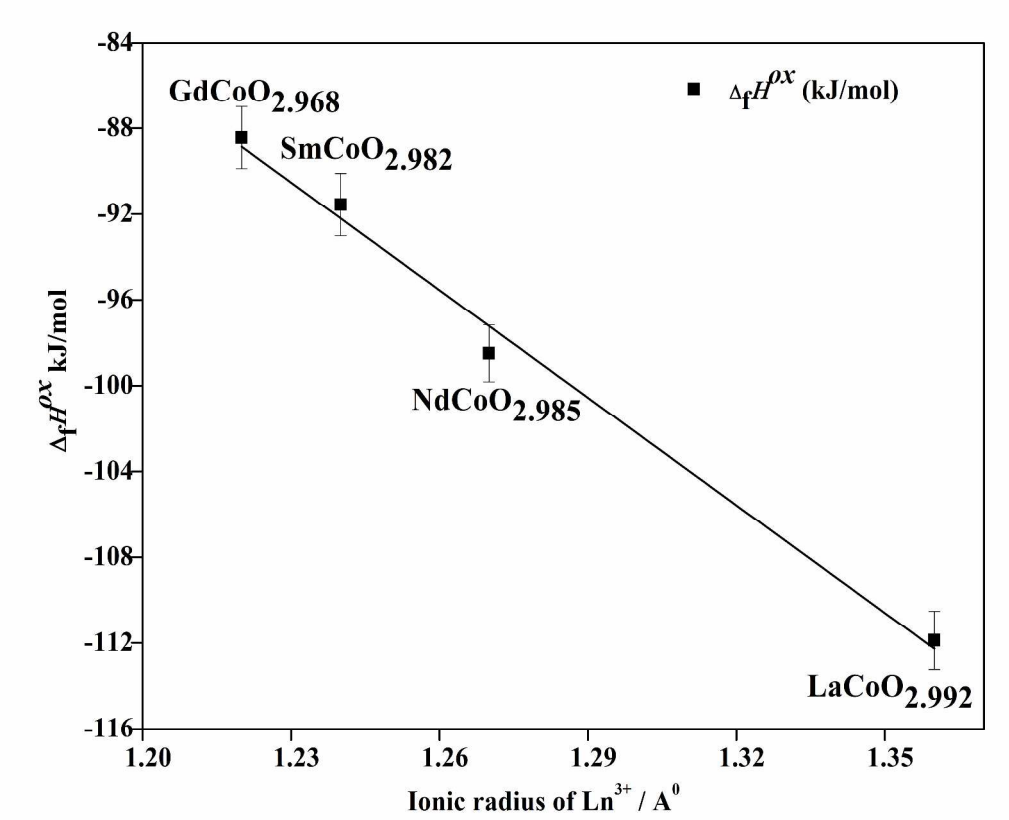

Figure 2 (b)

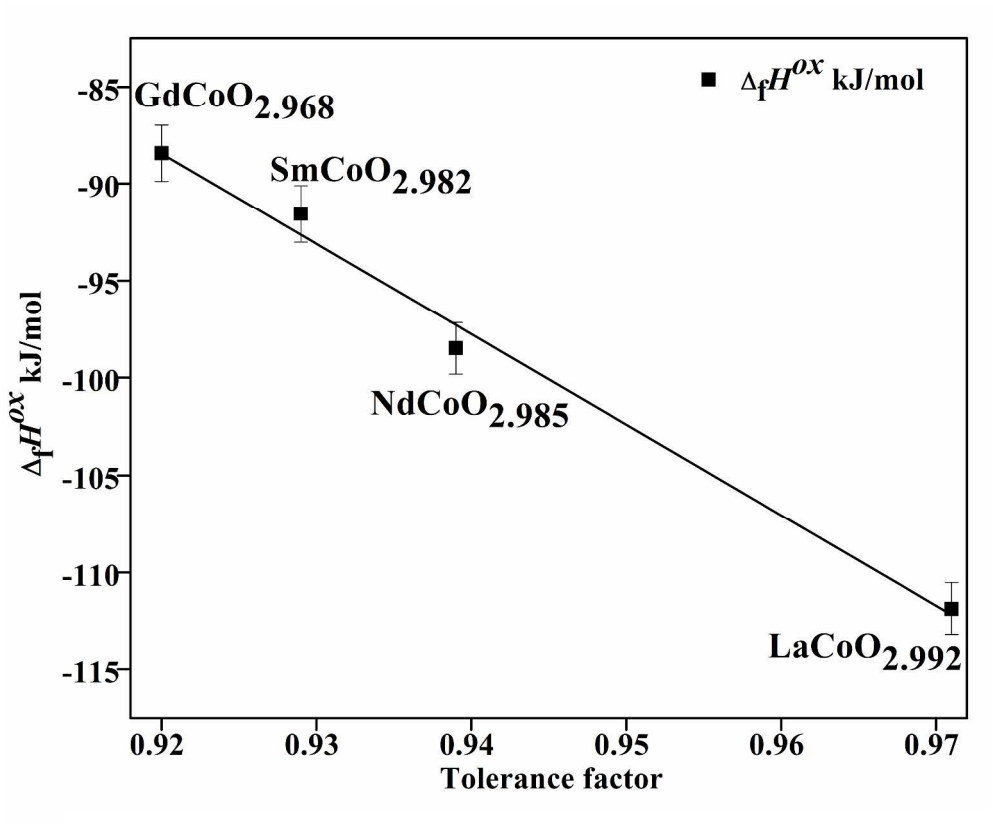

Graphical Abstract